electricity

MDPI

Article

Measurement and Evaluation of Voltage Unbalance in 2 × 25 kV 50 Hz High-Speed Trains Using Variable Integration Period

Yassine Taleb [1,*], Roa Lamrani [2] and Ahmed Abbou [1]

[1] EREEC Laboratory, Department of Electrical Engineering, Mohammadia School of Engineering, Mohammed V University in Rabat, Rabat 11000, Morocco; abbou@emi.ac.ma
[2] Advanced Systems Engineering Laboratory, National School of Applied Sciences (ENSA), Ibn Tofail University, Kenitra 14000, Morocco; roa.lamrani@uit.ac.ma
* Correspondence: yassinetaleb@research.emi.ac.ma

Abstract: This article addresses the need for a standardized method to measure power quality in railroad systems, which differ from distribution and transmission networks. It evaluates the applicability of existing standards in detecting variations and short-term disturbances in railroad networks powered by the 50/60 Hz AC grid or the 2 × 25 kV AC network used for high-speed trains. The objective is to propose a standardized algorithm capable of accurately identifying disturbances to assess power quality on railway traction substations. A new method is proposed to characterize voltage imbalances more precisely. Practical demonstrations confirm that a short integration period, as used in existing standards, provides a more accurate estimation of disturbance amplitude and duration. Field experiments validate the proposed solution, embedded in equipment installed on the 225 kV line supplying the 2 × 25 kV AC substation for high-speed rail. Comparative analysis of results obtained during high-speed train journeys confirms the algorithm's potential to aid standards committees in reviewing and updating existing standards, as well as expediting the creation, approval, and implementation of new standards for railway installations. Experimental comparisons of other power quality parameters, such as frequency and voltage harmonics, also underscore the algorithm's utility in railway power quality assessment.

Keywords: railway power supply systems; high-speed trains; power quality meter; EN 50160; power quality analyzer; voltage unbalance; current unbalance; voltage harmonics; frequency

Citation: Taleb, Y.; Lamrani, R.; Abbou, A. Measurement and Evaluation of Voltage Unbalance in 2 × 25 kV 50 Hz High-Speed Trains Using Variable Integration Period. *Electricity* **2024**, *5*, 154–173. https://doi.org/10.3390/electricity5010009

Academic Editors: Andreas Sumper and Eduard Bullich-Massagué

Received: 23 January 2024
Revised: 27 February 2024
Accepted: 29 February 2024
Published: 12 March 2024

1. Introduction

Rail infrastructure is essential to Morocco's national economy and forms the basis of transport systems in many countries. Electric railroads, particularly high-speed trains (HST), are becoming increasingly popular due to their advantages of fast, comfortable, and environmentally friendly transport. However, electric locomotives are single-phase loads [1], non-linear [2], rectifying [3], consuming reactive power [4], generating harmonics [5,6], resonances [7], and negative current and voltage sequences which are injected into traction power supply systems (TPSS) [8], and which can propagate onto the electrical power transmission network and then onto the public grid [9]. The performance of traction systems can be severely affected by these disturbances, including energy efficiency, the service life of electrical installation components [10], continuity of service, and the operational safety of the power system.

Power quality problems in railway applications are attracting increasing attention. The measurement, monitoring, and characterization of these phenomena [11] are particularly difficult due to their random and non-stationary nature. It should also be noted that power quality management in railway applications requires a global approach that takes into account all aspects of the traction system, including electrical equipment, control techniques, and operational control strategies.

There are not yet any standardized methods for measuring and evaluating power quality in the railway sector [12,13]. However, efforts are underway to establish such procedures. For example, some research and standardization organizations are working on methods to measure and characterize power quality phenomena in electric traction systems. These initiatives include the creation of simulation models, the collection of field data, and the study of the impact of power quality disturbances on traction system performance, and it is within the scope of these initiatives that this research work has been developed. These efforts are likely to result in the establishment of new standards or the modification of existing standards to take account of the specificities of the railway sector. Meanwhile, railway companies must refer to current best practices for monitoring and managing the quality of energy in their traction systems.

15 November 2018, saw the commissioning of substation N°1, which supplies electrical power to the high-speed trains linking KENITRA to TANGER over 175 km. This substation supplies power to 50% of the distance, representing 87 km, covered in 20 min, with trains traveling at a maximum speed of 320 km/h. The substation is connected to the 225 kV network via two 225 kV lines, LGV1 as the main line and LGV2 as the backup line. Figure 1 illustrates how the HSRs are connected.

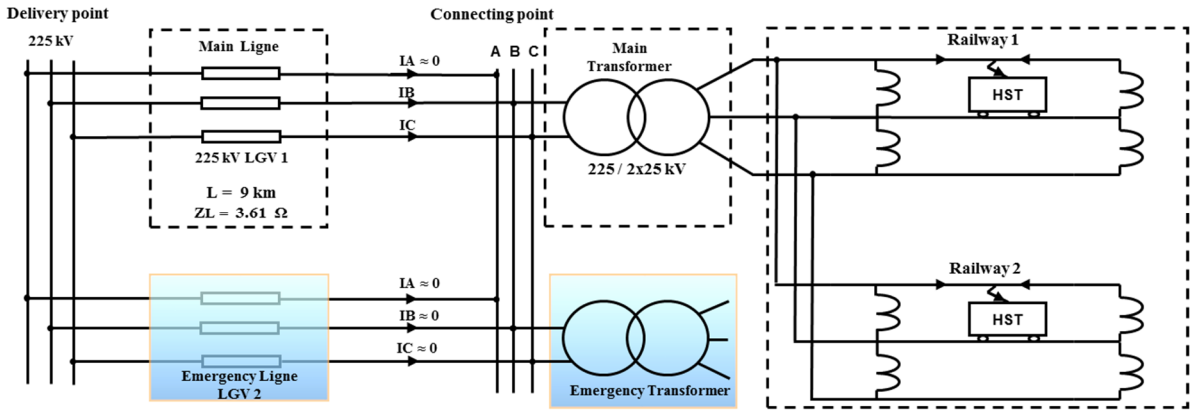

Figure 1. Multi-line diagram of a 2 × 25 kV-50 Hz single-phase AC substation.

A two-phase system supplies this type of train, which can negatively affect power quality due to electrical disturbances such as harmonics [6], voltage and current imbalances [8], overvoltage [14], and flicker [15]. An experimental study of the impact of harmonics and distorting power on the electrical grid and the energy recorded on a 25 kV AC network was reported in [11]. Then, a practical analysis based on an experimental study defining the interactions of harmonic currents from rank 1 to rank 50 between the 225 kV network and 2 × 25 kV AC railway substations supplying HSTs running at 320 km/h was discussed in [6].

Now, it is time to enrich the experimental database by analyzing the current state of voltage imbalances generated by 2 × 25 kV AC railway traction networks, to identify the weaknesses of the installed power quality meter and to improve measurement and acquisition techniques and algorithms in order to facilitate analyses and make their interpretation more reliable through values measured in the field.

The second part of this article will focus on studying the impact of voltage imbalance on various components of electrical systems such as generators, transmission lines, and connected loads. Then, it will be theoretically demonstrated that voltage imbalance is dependent on the active power demand and the short-circuit power.

In the fourth part, a quarterly recording from the main LGV1 line with Q80 power quality meters, based on the EN 50160 standard which is based on the measurement techniques described in the international standards IEC 61000-4-30 [16] and IEC 61000-4-7 [17], will be presented. The study will continue with the acquisition and evaluation of energy quality via a NIDAQ 6009 card [18], based on a variable integration period algorithm, installed in parallel with the SICAM Q80 for comparison and interpretation.

Finally, based on the presented results, it will be shown that the designed algorithm, which can be used to handle other energy quality parameters such as frequency and voltage harmonics, is capable of detecting random disturbances and identifying more precisely the interferences that may also appear in such systems.

It is worth pointing out that all the graphs illustrated in this paper reflect field measurements during high-speed train operation, involving total power consumption of 10 MW for single units consisting of 8 motors of 1 MW each, or even double units consuming 20 MW (16 motors).

2. Voltage Unbalance

2.1. Definition of Voltage Unbalance

A three-phase system is unbalanced when the three voltages are not equal in amplitude and/or are not 120° phase-shifted with respect to each other. The degree of unbalance is defined using Fortescue's component method by the ratio of the negative sequence (U1i) (or zero sequence (U1o)) of the fundamental to that of the positive sequence (U1d) of the fundamental. According to the international organizations, three definitions of voltage unbalance are stated.

- NEMA (National Equipment Manufacturer's Association) Definition

The NEMA definition [19] of voltage unbalance, also known as the line voltage unbalance rate (LVUR), is given by:

$$\%\text{LVUR} = \frac{\Delta UL \text{ dev}}{UL \text{ moy}} \times 100 \quad (1)$$

ΔUL dev: Maximum voltage deviation from the average line voltage.
UL moy: Average line voltage.

The NEMA definition assumes that the average voltage is always equal to the rated value, which is 480 V for the US three-phase systems, and since it works only with magnitudes, phase angles are not included.

- IEEE Definition

The IEEE definition [20] of voltage unbalance, also known as the phase voltage unbalance rate (PVUR), is given by:

$$\%\text{PVUR} = \frac{\Delta UP \text{ dev}}{UP \text{ moy}} \times 100 \quad (2)$$

ΔUP dev: Maximum voltage deviation from the average phase voltage.
UP moy: Average phase voltage.

The IEEE uses the same definition of voltage unbalance as NEMA, the only difference being that the IEEE uses phase voltages rather than line-to-line voltages. Here again, phase angle information is lost since only magnitudes are considered.

- True Definition

The true definition of voltage unbalance is defined as the ratio of the negative-sequence voltage component to the positive-sequence voltage component [21]. The percentage voltage unbalance factor (% VUF), or the true definition, is given by:

$$\%\text{VUF} = \frac{U2}{U1} \times 100 \quad (3)$$

$U2$: Negative-sequence voltage component.
$U1$: Positive-sequence voltage component.

2.2. The Impact of Voltage Unbalance

In a three-phase transmission system, the voltages are sinusoidal with equal amplitude and 120° phase shift. However, the resulting voltage system at the point of use may be unbalanced for a variety of reasons. The nature of unbalance includes unequal voltage amplitudes at the fundamental frequency, deviation of the fundamental phase angle, and different levels of harmonic distortion between phases [22].

The main cause of voltage unbalance is the irregular distribution of single-phase loads, which can vary continuously across a three-phase system. Rural electrification, with its extensive distribution lines, is one example of unbalanced loads, as are loads for street lighting in towns and cities. In our case, the two-phase load for traction may be a considerable cause of the perceived unbalance in the three-phase system since the system is supplied by only 2 phases VL2L3 = 225 kV.

Voltage unbalance could produce various effects on the transmission system and the equipment, as is the case with induction motors and power electronics converters, emphasized by the fact that a small voltage unbalance may cause a large phase current unbalance. Under unbalanced conditions, the transmission system will be subjected to higher losses, heating effects, and less stability, because when phases are unbalanced, the system is better placed to respond to unexpected power transmissions [23].

One of the crucial constraints affecting large two-phase loads, such as tensile loads, is to keep the value of the negative-sequence voltage (NPS) within acceptable limits.

High NPS voltage values slightly lower the control of asynchronous motors and excessively increase rotor heating in such machines.

Voltage unbalances affect all three-phase equipment, causing oscillations on the DC bus of three-phase converters [24,25]. It generates power losses in distribution lines (T.-H. Chen 1995) [26], and, in particular, in motors [27], as these are subjected to an undesirable braking torque, which results in overheating, a consequent degradation of electrical insulation and a reduced lifetime. Any voltage unbalance over 1% causes overheating of the equipment, which means that it must be oversized to compensate for this overheating and avoid premature degradation.

Negative sequence (or zero sequence) voltage is caused by:

- Voltage drops along grid impedances due to negative (or zero-sequence) currents produced by unbalanced loads, leading to non-identical currents on all three phases [28];
- Transients from the railway power system (Tsai-Hsiang 1994) [29];
- Voltage unbalance from voltage sources (Kersting 2010) [30].

The most commonly used techniques for reducing voltage unbalance are based on balancing the loads on each phase; it should be said here that only the unbalance caused by these loads is reduced. Some examples of these techniques are shown below:

- The elimination of current unbalance by canceling the negative sequence without consuming active power (Bhavaraju and Enjeti 1993) [31].
- Load balancing using shunt compensators (Ghosh and Joshi 2000) [32].
- Applications for four-wire non-sinusoidal interphase load balancing using instantaneous power theory (Chen and Hsu 2000) [33].

2.3. The Effect of Voltage Unbalance on the HV Transmission Network

The main function of a transmission network is to efficiently deliver electrical energy to different destinations for use by customers. The negative sequence contributes, along with other factors, to the unbalance of currents, which means the presence of a negative sequence [34]. In practice, the current negative sequence does not allow power transmission; this is because it is orthogonal to the positive-sequence voltage. However, it increases line losses and raises conductor heat. Thus, the current negative sequence reduces the power transmission capacity of transmission networks [23].

One of the requirements for supplying two-phase loads is to keep the level of unbalance below 1%.

For example, for a load of between 50 MW and 100 MW, the supply system should have a short-circuit power between 5 GVA and 10 GVA to meet voltage unbalance requirements. In many circumstances, the traction system is relatively far from the short-circuit power levels ensured by HV supply lines.

Given this multitude of consequences, extensive research into railway networks and the provision of real, accurate measurements seemed to be a priority.

3. Two-Phase Power System Configuration for an HST-Type Load

3.1. System Description

The two-phase power supply is a system used to supply electricity to high-speed trains (HSR) in MOROCCO. It uses two current-shifted phases to supply the 225/2 × 25 kV AC railway traction substations. In Morocco, only phases B and C are supplying the substations, while phase A remains unloaded.

In the 2 × 25 kV AC system, power from the substations is transmitted to the trains via the feeder and catenary systems. Substations use an autotransformer with a mid-point secondary winding. The feeder autotransformer is connected to one of the transformer's secondary terminals, and the catenary is connected to the other terminal of the winding. The midpoint of the secondary winding is connected to the earth and rail.

3.2. Power System Diagram

The present case study analyses the two-phase system supplying the high-speed railway of 2 × 25 kV 50 Hz system. The project is made up of two substations and ten stations for paralleling autotransformers according to the diagram in Figure 2.

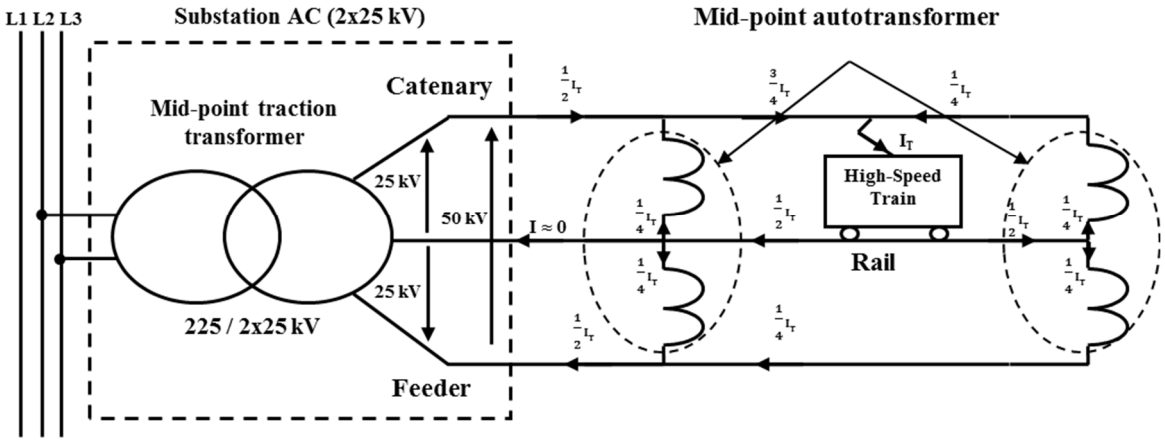

Figure 2. Connecting diagram between two phases of an HSR substation.

Establishing the relationship between the power amplitude of a two-phase load, the three-phase short-circuit power at the common connection point, and the modulus of the negative sequence of the voltage system.

3.3. Definitions

- E1: Phase-to-neutral positive sequence of the FEM source.
- IA: Phase "A" current.
- IB: Phase "B" current.
- IC: Phase "C" current.
- Ich: Single-phase load current, flowing through phases "B" and "C".
- Id: Positive sequence of current.
- Ii: The negative sequence of the current.
- Ih: The zero sequence.

$$a = -\frac{1}{2} + j\sqrt{\frac{3}{2}},\ the\ e^{j120^\circ}\ operator. \tag{4}$$

Consider a single-phase load supplied from two phases of a three-phase system. We take Zch as the impedance, and Vm as the voltage at the load's midpoint Zch, as shown in Figure 3:

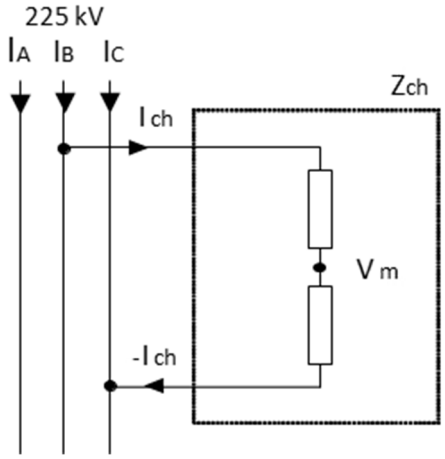

Figure 3. Equivalent two-phase load model (substation and high-speed train).

Applying FORTESCUE's Theorem allows for the decomposition of any unbalanced three-phase system into positive, negative, and zero sequence system sums.

$$I_A = I_d + I_i + I_h = 0 \tag{5}$$

$$I_B = \mathrm{a}^2\, I_d + \mathrm{a} I_i + I_h = I_{ch} \tag{6}$$

$$I_C = \mathrm{a} I_d + \mathrm{a}^2\, I_i + I_h = -I_{ch} \tag{7}$$

$$\mathrm{a}^2(E_1 - I_d Z_d) - I_i Z_i - I_h Z_h = 0.5 Z_{ch}\left(\mathrm{a}^2 I_d + \mathrm{a} I_i + I_h\right) + V_m \tag{8}$$

$$\mathrm{a}(E_1 - I_1 Z_1) - \mathrm{a}^2 I_i Z_i - I_h Z_h = 0.5 Z_{ch}\left(\mathrm{a} I_d + \mathrm{a}^2 I_i + I_h\right) + V_m \tag{9}$$

Adding Equation (5) to (7) gives $I_h = 0$, and Equation (1) gives $I_d = -I_i$.
Replacing I_i in Equations (6) and (7), and subtracting Equation (7) from Equation (6), gives:

$$\left(\mathrm{a}^2 - \mathrm{a}\right) I_d = -\mathrm{j}\sqrt{3} I_d = I_{ch} \tag{10}$$

Also, subtract Equation (9) from Equation (8) to obtain:

$$E_1 - I_d Z_d - I_d Z_i = Z_{ch} I_d \tag{11}$$

For a single-phase load (P, Q), where P is the active power and Q is the reactive power, we have the following:

$$\mathrm{P} + \mathrm{jQ} \approx E_1\left(\mathrm{a}^2 - \mathrm{a}\right) I_{ch}^* \tag{12}$$

where * is the conjugate.

By replacing Ich using Equation (10), Equation (12) can be reformulated as follows:

$$(\mathrm{P} - \mathrm{jQ})\left(E_1^*\left(\mathrm{a} - \mathrm{a}^2\right)\right) - 1 \approx \left(\mathrm{a}^2 - \mathrm{a}\right) I_d \tag{13}$$

$$I_d \approx (\mathrm{P} - \mathrm{jQ})\left(E_1^*\left(\mathrm{a} - \mathrm{a}^2\right)\left(\mathrm{a}^2 - \mathrm{a}\right)\right) - 1 = (\mathrm{P} - \mathrm{jQ})(3E_1^*) - 1 \tag{14}$$

This implies that, for a load, the current's positive sequence is the same, regardless of whether the load is a balanced three-phase load or a single-phase load connected between phases.

By replacing I_d with $-I_i$ in Equation (14), the voltage's negative sequence (NPS) is obtained:

$$I_i Z_i \approx -(\mathrm{P} - \mathrm{jQ})(3E_1^*) - 1Z_i \tag{15}$$

Subsequently, the voltage's negative sequence (NPS) is expressed in PU with respect to the nominal voltage E_1:

$$I_i Z_i(E_1) - 1 \approx -(\mathrm{P} - \mathrm{jQ})(3E_1\ E_1^*) - 1Z_i \quad \text{in PU} \tag{16}$$

In general, $Z_i << Z_d$, but when far from generation sources, $Z_i \approx Z_d$, so a slight error by an excess of the voltage's negative sequence in PU compared to the nominal value of the voltage's positive sequence is given by:

$$I_i Z_i(E_1) - 1 \approx -(\mathrm{P} - \mathrm{jQ})(3[E_1]^2) - 1Z_d \quad \text{in PU} \tag{17}$$

But $(3[E_1]^2) - 1\ Z_d$ is the short-circuit power level, while $(\mathrm{P} - \mathrm{jQ})$ is the conjugate of the load's complex power. Therefore, the amplitude of the voltage's negative sequence in PU is equal to the following:

$$V_i = \frac{\sqrt{(P^2 + Q^2)}}{\left(3[Ed\ ]^2\right) Zd^{-1}} \tag{18}$$

The voltage imbalance is, therefore, equal to the ratio of the single-phase apparent power to the short-circuit apparent power.

4. Power Quality Measurement Based on EN 50160

EN 50160 is a European standard that establishes specifications for power quality in distribution and transmission networks. It defines the characteristics of electrical voltages in low-voltage, medium-voltage, and high-voltage networks.

Based on this standard, the suggested algorithm consists of the following basic steps:

1. Measurement structure

The electrical parameter to be measured can be either directly available, which is generally the case for low-voltage networks, or available via measurement transducers for medium- and high-voltage networks.

The complete measurement chain is illustrated in Figure 4.

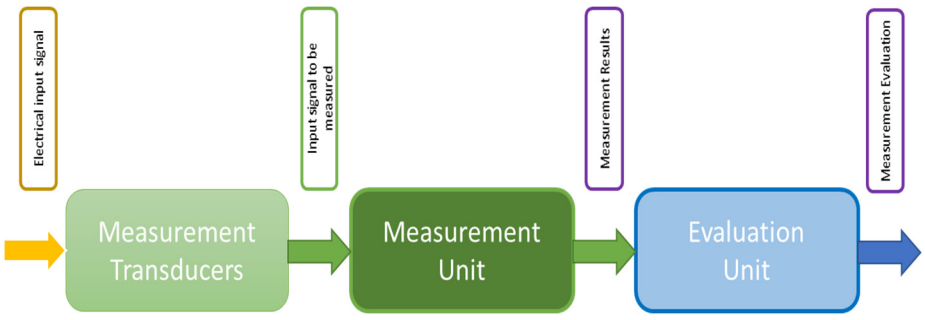

Figure 4. Block diagram of measurement.

A measuring instrument generally includes the entire measurement chain.

In EN 50160, the normative part does not take into account transducers or the measurement uncertainty they introduce.

2. Electrical values to be measured

Measurements can be taken on single-phase or polyphase networks. Depending on the context, it may be necessary to measure voltages between phase conductors and neutral (phase-neutral), or between different phase conductors (phase-phase), or between neutral and earth. The standard is not intended to impose a choice.

3. Integration of measurement time intervals

A time interval for measuring amplitudes (network voltage, harmonics, interharmonics, and unbalance) must be 10 periods for a 50 Hz network or 12 periods for a 60 Hz network.

Note that the uncertainty of this measurement is included in the test procedure associated with each parameter.

Measurement time intervals are integrated according to three values:

- Interval of 150/180 periods (150 periods for a nominal frequency of 50 Hz or 180 periods for a nominal frequency of 60 Hz),
- Interval of 10 min,
- Interval of 2 h.

4. Measurement integration process:

Integrations are calculated by the square root of the arithmetic mean of the square of the input values.

Three types of integration are required:

- Integration of periods: Data from the 150/180-period interval must be integrated from fifteen 10/12-period intervals.
- Integration of periods in clock time: Values at 10 min will be identified with an absolute date (e.g., 01H10.00). This date corresponds to the end of the 10 min integration period. If the last 10/12 period value of a 10 min integration overlaps with the absolute boundary of the 10 min, this 10/12 period value is included in this 10 min integration.
- When measurements are started, a 10/12-period interval must begin with an absolute 10 min boundary and must be successively resynchronized at each absolute 10 min mark.
- Clock time integration: The "2 h interval" data should be aggregated from twelve 10 min intervals.

5. Parameter Calculations According to EN 50160

Figure 5 shows the part of the code that calculates the parameters according to the evaluation method specified in standard EN 50160. There are three types of parameters:

To accurately calculate the parameters as defined by the EN 50160 standard, specific methodologies are applied for each power quality attribute. Here is a brief overview of the calculation methods for some of the key parameters:

Network Frequency Calculation:

Frequency is determined by measuring the number of cycles of the waveform per unit of time, typically over a 10 s interval. The average frequency is then compared against the standard range.

Supply Voltage Variations:

Voltage variations are calculated by taking RMS (root mean square) voltage measurements over 10 min periods.

Rapid Voltage Changes & Flicker:

The flicker severity is quantified using the Pst (short-term flicker severity) and Plt (long-term flicker severity) indices. These indices are calculated based on the fluctuation of the voltage level over 10 min for Pst and 2 h for Plt, assessing the impact of voltage fluctuation on the light flicker perceived by the human eye.

Voltage Dips:

Voltage dips are identified by measuring the depth and duration of any voltage reduction below a predefined threshold. The characteristics of these dips are typically analyzed for events with durations less than 1 s and depths less than 60%.

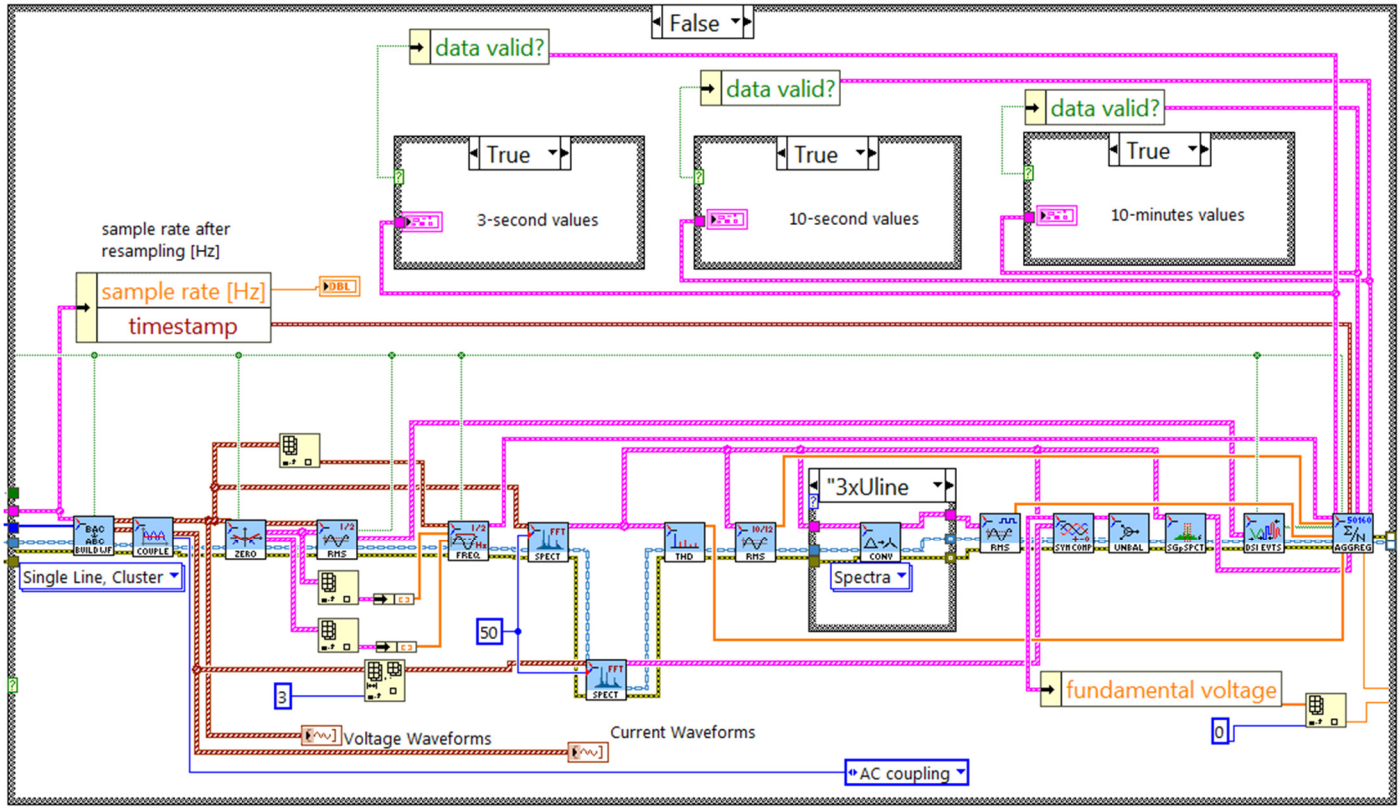

Figure 5. Measurement calculation and integration block.

Short and Long Interruptions:

Interruptions are categorized based on their duration. Short interruptions are those lasting less than 3 min, and long interruptions last more than 3 min. The frequency and duration of these interruptions are recorded over a week to assess compliance with the standard.

Overvoltage:

Overvoltage is measured as instances where voltage exceeds the nominal voltage by a certain threshold. The measurement criteria are not explicitly defined but involve identifying peak voltage levels that surpass the normal operating range.

Voltage Unbalance:

Voltage unbalance is calculated using the formula:

$$V_{unb} = \frac{Vmaxdeviation}{Vaverage} \times 100 \quad (19)$$

This involves measuring the phase-to-phase voltages, calculating the average, and then determining the maximum deviation from this average. The unbalance is then expressed as a percentage.

Harmonics and THD:

Harmonic distortion is calculated by measuring the harmonic components of the voltage waveform and their contribution to the overall waveform distortion. The Total

Harmonic Distortion (THD) is calculated as the ratio of the sum of the powers of all harmonic components to the power of the fundamental frequency component.

For each parameter, the integration period over which measurements are taken and calculations are performed is crucial for ensuring that the assessments are in line with EN 50160 requirements. These methodologies provide a structured approach to monitoring and ensuring power quality within the specified limits of the standard.

- Parameters calculated every 3 s are displayed in the "3-s values" section.
- Parameters calculated every 10 s are displayed in the "10-s values" section.
- Parameters calculated every 10 min are displayed in the "10-min values" section.

The recording of voltage imbalance over three months is shown in Figure 6.

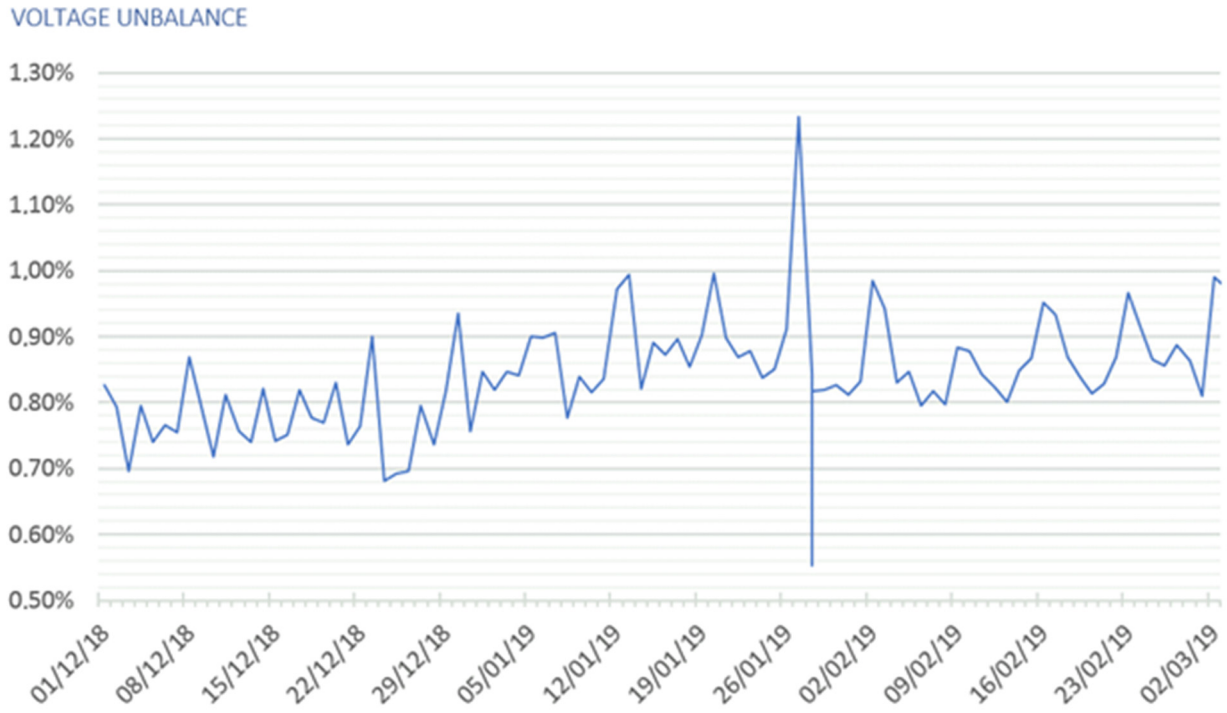

Figure 6. Three-month record of daily maximums of voltage unbalance.

Figure 6 shows a record from 1 December 2018 to 2 March 2019 of the maximum daily rates of negative-sequence voltage unbalance recorded by the Q80 power quality meter, which exceeded the limit value required by standard EN 50160, which is 1%.

Without taking this maximum into account, the mean of the integrated voltage unbalance maximums over 10 min is around 0.85%.

Given that traffic during this period has a 1 h interval between each departure of HSTs with single-unit operation, these rail networks have to withstand considerable current calls due to the growth in daily traffic.

When two or more trains cross the same feeder sector, the sub-stations supplying the HSTs will be subjected to a large load demand, resulting in load calls as large as those recorded during this quarter.

To validate the relationship between voltage imbalance and power demand at the substation, the voltage imbalance graph for the day of 27 January 2019 had to be plotted on top of the load curve for the same day to confirm the above-mentioned theoretical study. The recording of voltage unbalance and power demand on the LGV1 line on 27 January 2019 is shown in Figure 7.

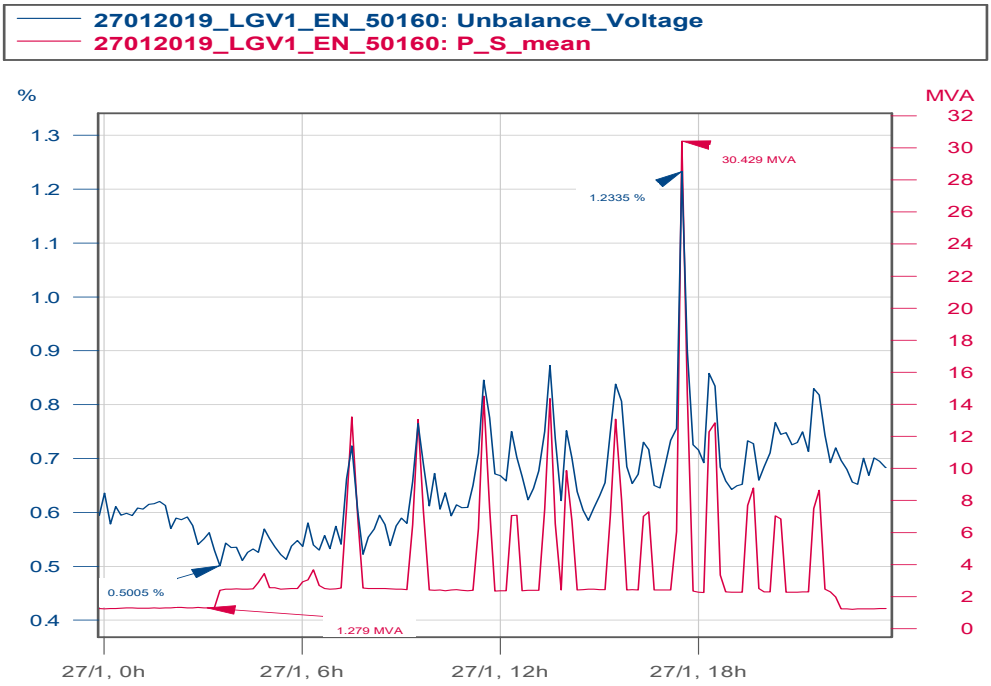

Figure 7. Substation voltage imbalance and apparent power of 27 January 2019.

Figure 7 may reflect the following:

- The blue graph represents the voltage imbalance, which varies between 0.5% and 1.2% during the day, while the red graph illustrates the power drawn by high-speed trains during the same day. The graphs for the 2 parameters have the same shape, confirming the theory mentioned above.
- During the high-speed train stop at night, from 00:00 to 5:00, the imbalance rate varies between 0.5% and 0.62%. This interval is explained by the imbalance of the HV network associated with the unloaded rail traction substation.
- At the start of HST traffic, this rate varies between 0.7% and 0.85% and follows the power demand of single-unit trains with an average power of 16 MVA.
- Furthermore, the graph also indicates that voltage imbalances exceed expected levels during the crossing of double-unit high-speed trains (TGVs) on tracks powered by the same substation, attributable to a power consumption of 30 MVA.
- While rail networks are not governed by a standard, and the impact of the negative sequence voltage imbalance mentioned above requires rigorous monitoring, the integration periods on current power quality meters do not allow for the detection of transient and quasi-stationary phenomena.

6. Power Quality Measurement Based on the Proposed Algorithm

The various components used, and the programming tools required to create the graphical interface, are presented in this section.

1. System architecture

The solution consists of:

- A step-down module containing three voltage transformers (VT) and three current transformers (CT) to reduce input voltages and currents;
- An anti-aliasing filter module, which mainly filters out the values from the voltage transformers (TT) and current transformers (CT) to reduce the input voltages and currents;
- A processing board that mainly converts the electrical input signal into an electrical signal that can be used by the processing unit;
- An acquisition board that performs the analog-to-digital conversion and calculation of the parameters required to evaluate the PQ parameters with a variable integration period;

- A graphic interface to visualize the results obtained.

Figure 8 shows the connection of the Q80 qualimeter based on the EN 50160 standard in the black rectangle, and the designed equipment in the blue rectangle, with the elements making up the solution, and including the variable integration period power quality evaluation algorithm.

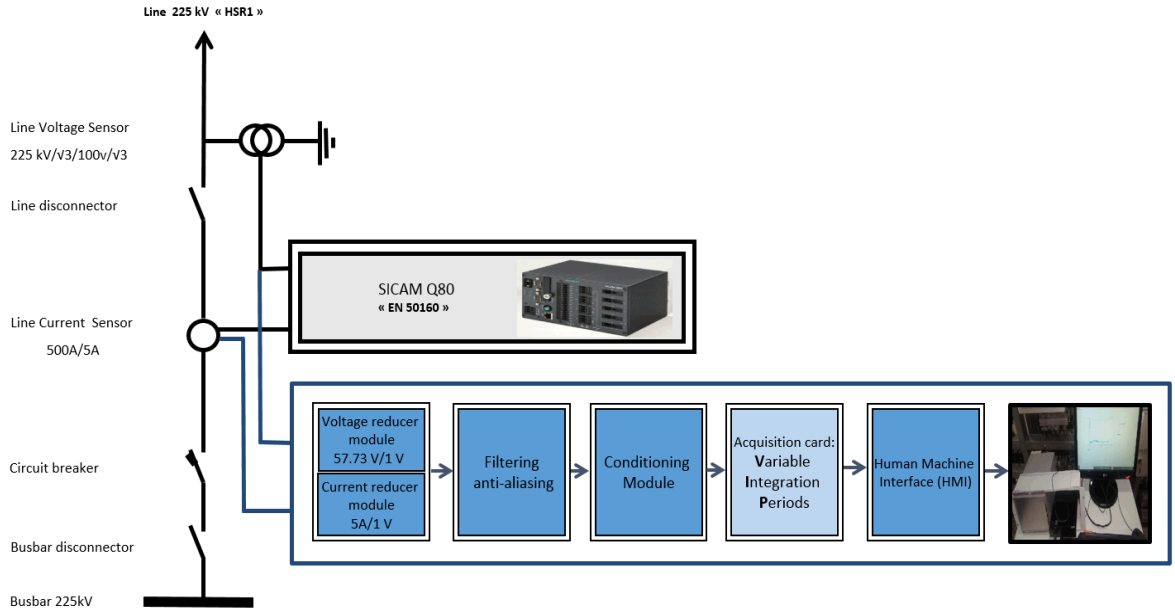

Figure 8. Power quality meter architecture incorporating the variable integration period.

On the acquisition board, and specifically on the power quality parameter integration period calculation block, a 1 s integration period has been introduced to accurately visualize the evolution of voltage unbalance on 2 × 25 kV AC traction networks (Figure 9).

To demonstrate the ability of such an algorithm to accurately detect variations in electrical parameters and disturbances on 2 × 25 kV 50 Hz rail traction networks, it was commissioned on 23 October 2021 from 00:00 to 15:30, in parallel with the existing power quality meter.

A presentation of the recordings over 7 train trips of the two different devices, as well as an experimental comparison of the results, will justify the benefits of the new algorithm, illustrated on Figure 9.

The process begins with sampling electrical magnitudes, specifically three-phase voltages from voltage transformers, crucial for capturing data for analysis. Each power quality parameter is calculated in separate blocks using data sampled at 48 kb/s for precision.

At this phase, acquired measurements are directed to an averaging calculation block, which allows for the setting of the integration period from 1 s up to 10 min, offering electrical network analysis experts flexibility based on the rapid or slow variation of the parameter being evaluated. The calculation results are recorded and displayed on the graphical interface for real-time visualization and historical tracking. Instant parameter evaluation detects any deviations from pre-established limit values.

To mathematically demonstrate the benefit of equipping a power quality meter with a variable integration period over a fixed one, specifically for evaluating voltage imbalance, consider the formula for voltage imbalance in a three-phase system. The voltage imbalance (V_{unb}) is often calculated as a percentage of the average voltage and the maximum deviation from this average:

$$V_{unb} = \frac{Max(|V1 - Vavg|, |V2 - Vavg|, |V3 - Vavg|)}{Vavg} \times 100 \quad (20)$$

$V1$, $V2$, and $V3$ are the phase voltages, and *Vavg* is the average of these three voltages.

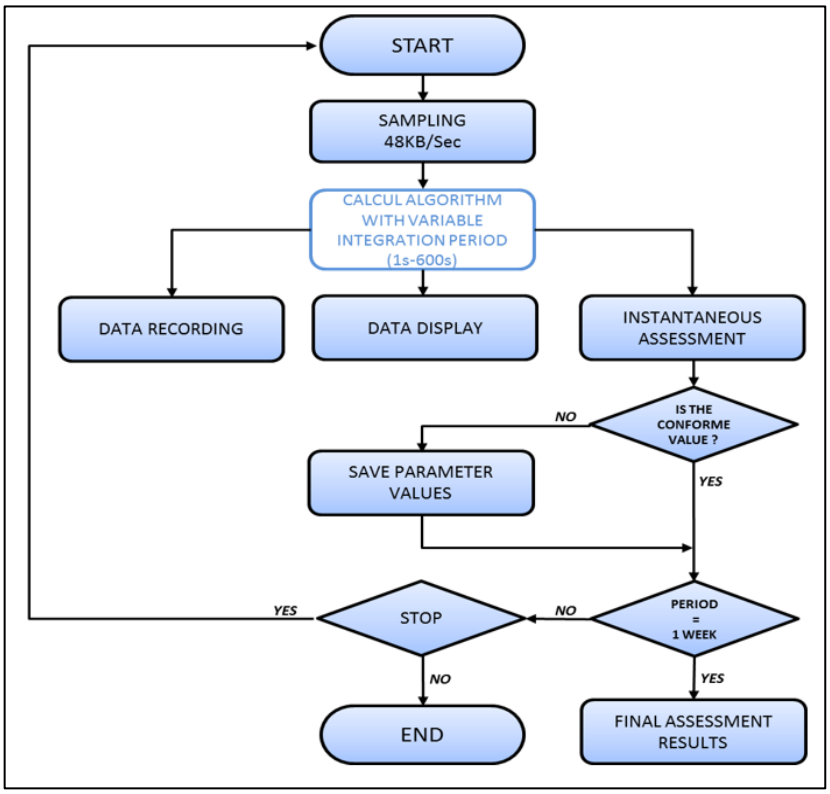

Figure 9. Measurement algorithm with variable integration period.

A variable integration period allows for adjusting the calculation window to capture transient imbalances that a fixed period might miss. For transient or fluctuating loads, a shorter period could detect rapid changes more accurately. Conversely, for stable conditions, a longer period could average out minor fluctuations, providing a clearer picture of sustained imbalances. This adaptability ensures a more accurate assessment of voltage quality, crucial for maintaining power system reliability and efficiency.

This solution ensures continuous monitoring and adapts to user needs while maintaining data integrity and compliance, with detailed attention to flexible integration periods and precise data handling.

2. Visualization and comparison of voltage imbalance recordings

Figure 10 shows the voltage imbalance recorded on the LGV1 line on 23 October 2021 from 00:00 to 15:30, measured over 7 train journeys.

Figure 11 showcases a zoomed-in view of the area framed in red between 07:00 and 09:00, specifically illustrated to closely examine the graph's trends. This thorough observation aimed to validate the accuracy of the negative sequence voltage imbalance rate achieved through the proposed algorithm. The enlargement of this specific time range allows for a detailed analysis of the graph's trends, highlighting the algorithm's effectiveness and performance in accurately measuring negative sequence voltage imbalances. This detailed scrutiny ensures the algorithm's reliability and efficiency in real-world applications.

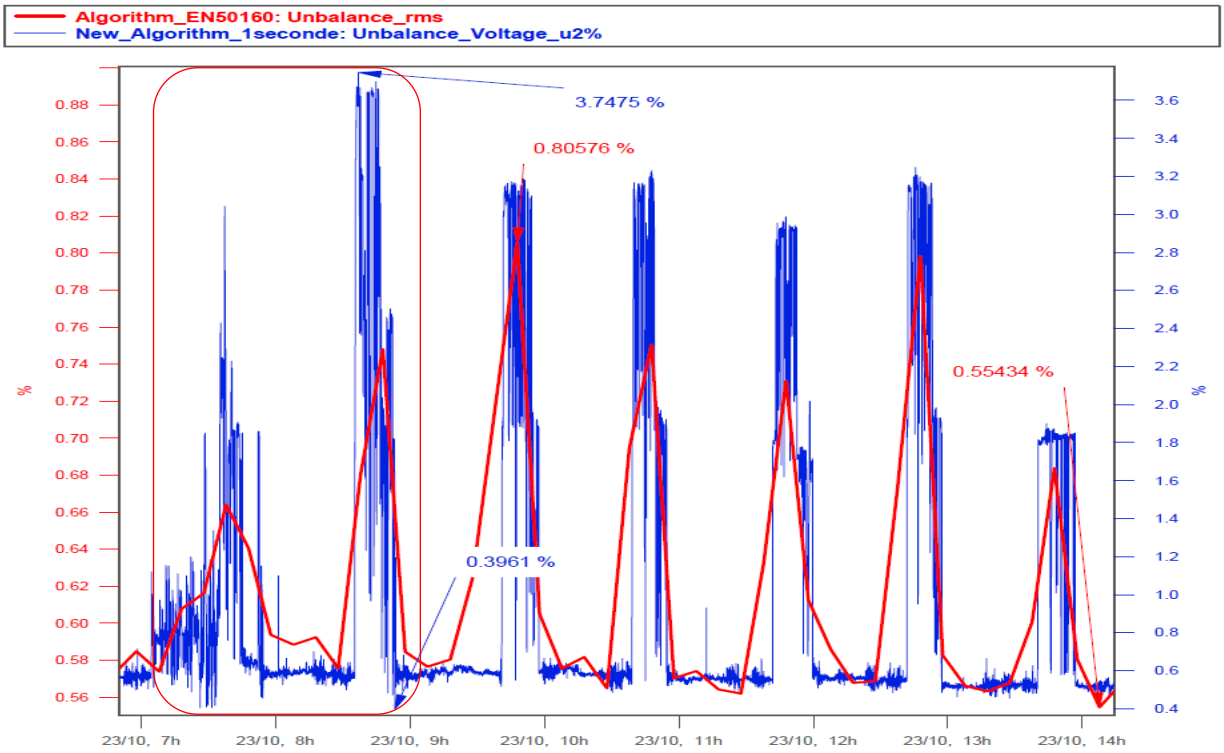

Figure 10. Voltage imbalance recorded on 7 trips.

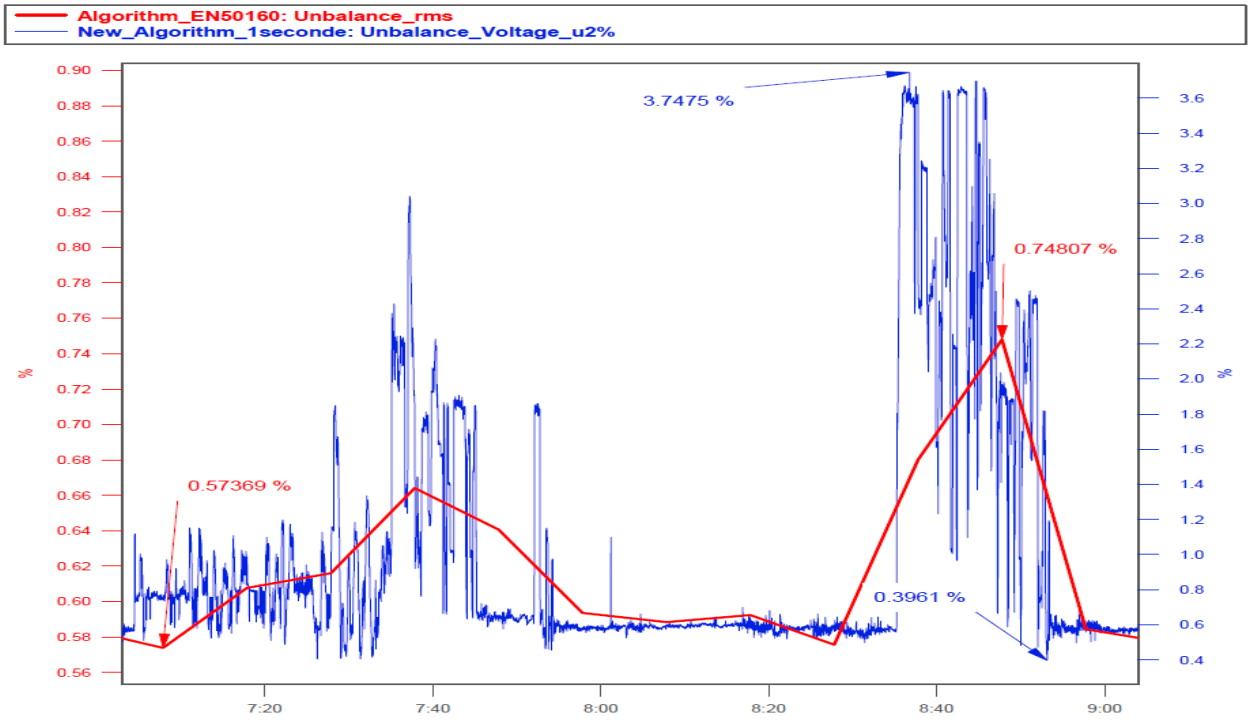

Figure 11. Voltage imbalance recorded on 2 trips.

The first trip of 7:00 a.m. corresponds to the scan train, which performs the daily test of the condition of the entire rail–catenary–locomotive system, with a maximum speed of 200 km/h. The maximum voltage imbalance recorded by the new algorithm is 0.82%, while the average calculated over 10 min is 0.66%.

The graphs in red illustrate the voltage imbalance provided by the device based on standard EN 50160, integrated over 10 min, while the graphs in blue represent the curve elaborated by the new algorithm, integrated over 1 s.

The second recording, at 8:35 a.m., represents the operation of a double-unit train traveling at a maximum speed of 320 km, resulting in a maximum voltage imbalance of 3.75%.

Recording over such a short integration period confirms the data abundance and the ability of the new algorithm to detect short-duration variations, enabling judicious precision and accurate judgment.

To verify the impact of the operating modes of high-speed trains (TGV) on the variation of the voltage imbalance rate, the proposed solution also allows for the recording of active, reactive, and apparent power, which will facilitate the analysis. To do this, it was necessary to overlay its graph in "blue" on that of the apparent power consumed in "red" by the TGV over the same course.

Based on the analysis of the graphs in Figure 12, it is observed that:

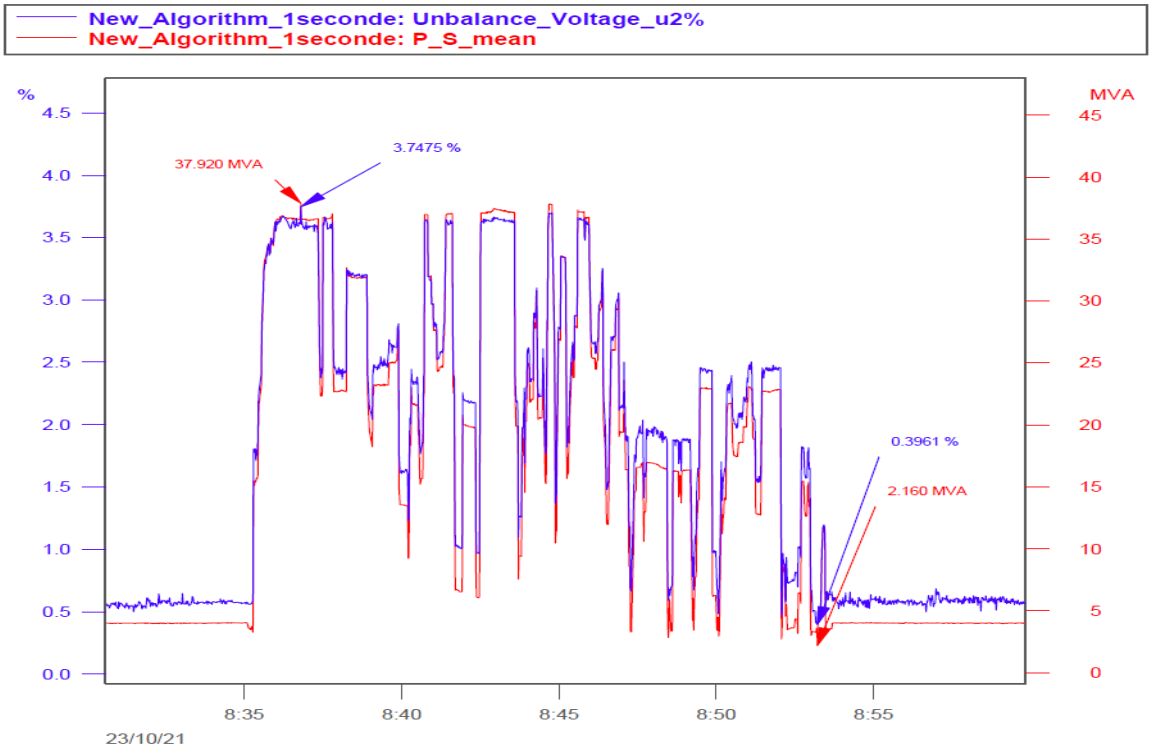

Figure 12. Substation voltage imbalance and apparent power with the new algorithm.

The minimum apparent power consumed by the TGV is 2.160 MVA, while the maximum apparent power reaches 37.92 MVA.

The voltage imbalance rate (u0% Voltage) shows a minimum value of 0.3961% and a maximum value of 3.7475%.

The coincidence of these values at the same moments suggests that the consumption of apparent power is responsible for the significant variation in the voltage imbalance rate during the different operational modes of the TGV (acceleration, cruising speed, deceleration, and braking), which justifies the cited theory.

The variation in apparent power is substantial, indicating significant changes in power demand across these modes. The voltage imbalance rate varies within the observed range, potentially reflecting the impact of TGV operational modes on energy quality.

3. Visualization and comparison of voltage harmonic rate recordings

Figure 13 shows the voltage harmonic rate recorded on the LGV1 line on 23 October 2021 from 03:00 to 09:00.

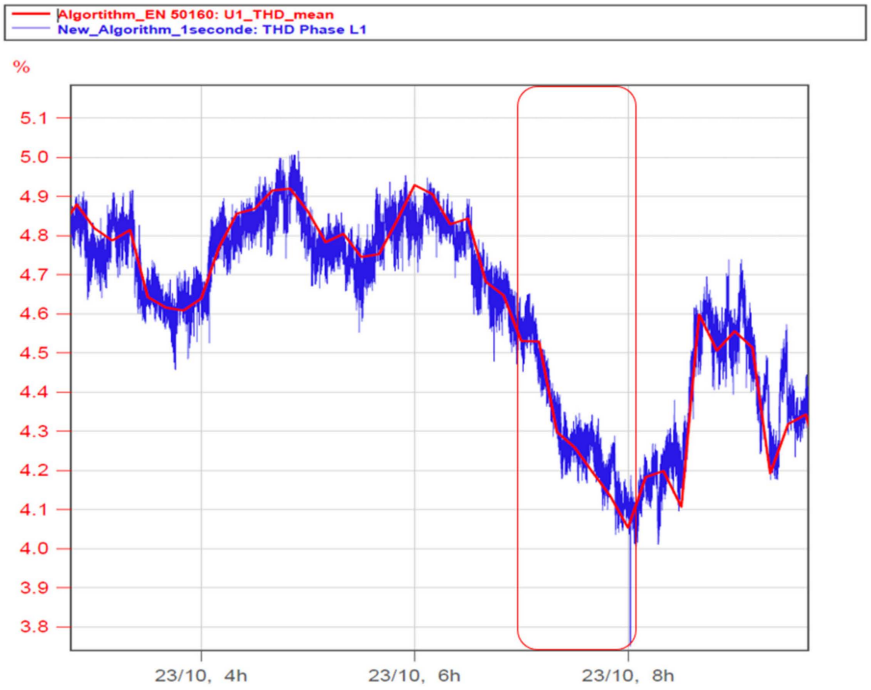

Figure 13. Average harmonic rate of U1 voltage (EN 50160 vs. new algorithm).

The area framed in red from 07:00 to 08:00 was zoomed in on in Figure 14 to facilitate a thorough examination of the graph's trends and to confirm the accuracy of the voltage harmonic distortion rate acquisition. This will simplify the determination of the suitable integration period for assessing this parameter, which is based on its time variation. This approach ensures a balance between accuracy and storage.

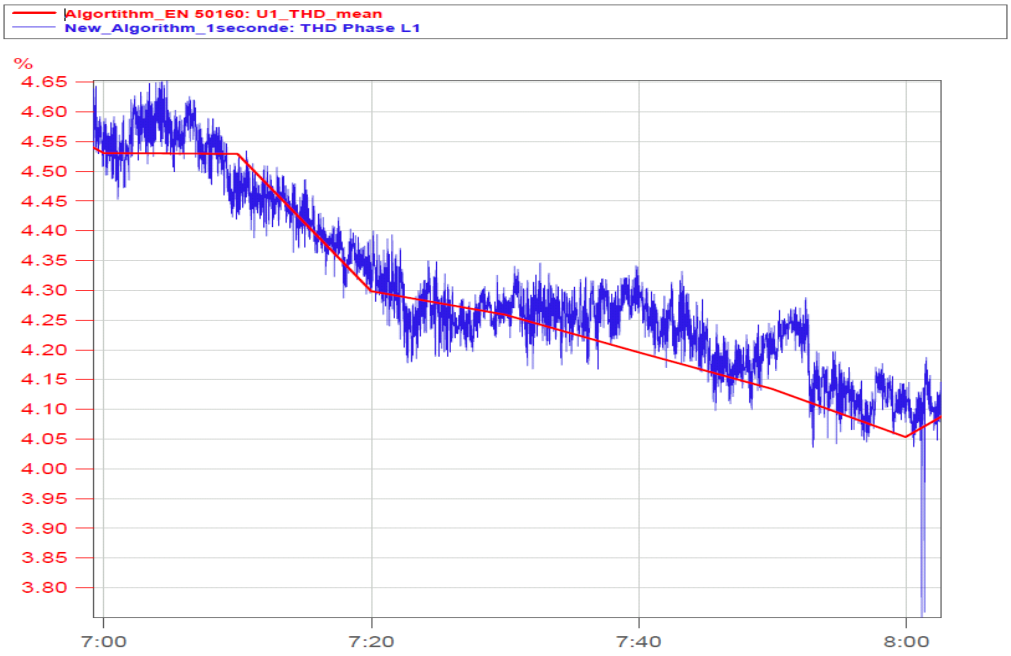

Figure 14. Average harmonic rate of U1 voltage recorded (Zoom).

The graphs in red illustrate the average voltage harmonic rate recorded based on the EN 50160 standard, integrated over 10 min, while the graphs in blue represent the curve developed by the new algorithm.

Figure 13 shows that the average voltage THD measured over 6 h of the same day varies between 4.1% and 5%, which is in line with the EN 50160 standard.

Given that the variation of this parameter is slower than that of the voltage unbalance, it can be seen that the two graphs have the same appearance, except that, for the proposed algorithm, a minimum of 3.75% recorded at 08 h 01 min could be detected.

4. Visualization and comparison of frequency recordings

Figure 15 shows the frequency recorded on the LGV1 line on 22 October 2021 from 18:00 to 00:00.

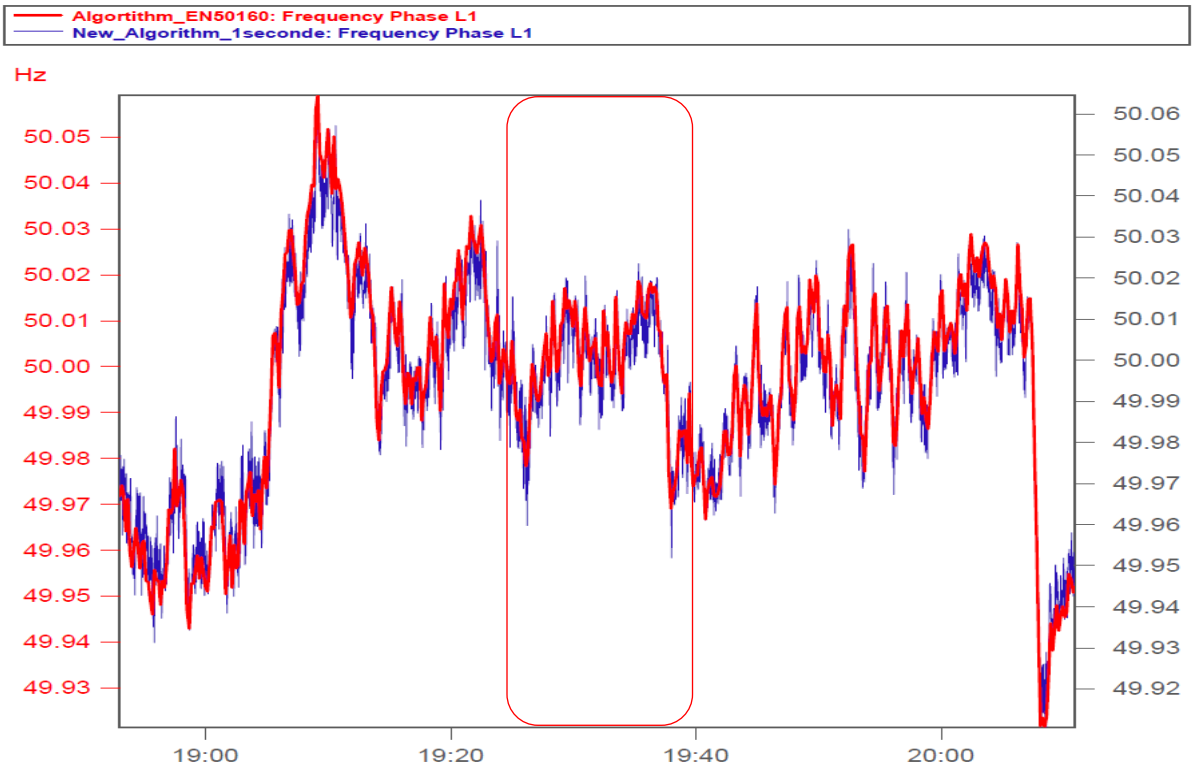

Figure 15. L1 voltage frequency recording (EN 50160 vs. new algorithm).

The red box from 19:25 to 19:40 has been zoomed in on Figure 16 to better visualize the trends of the graphs, and also to demonstrate the frequency acquisition capacity of the frequency phase L1 by the proposed solution.

The graphs in red illustrate the L1 voltage frequency recorded based on the EN 50160 standard, integrated over 10 s, while the graphs in blue represent the curve elaborated by the evaluation integrated at 1 s.

Figure 15 shows that the frequency of the L1 voltage measured over 6 h varies between 49.91 Hz and 50.06 Hz, which is in line with the EN 50160 standard.

Since the EN 50160 integration is performed over 10 s, it can be seen that both graphs show the same trend.

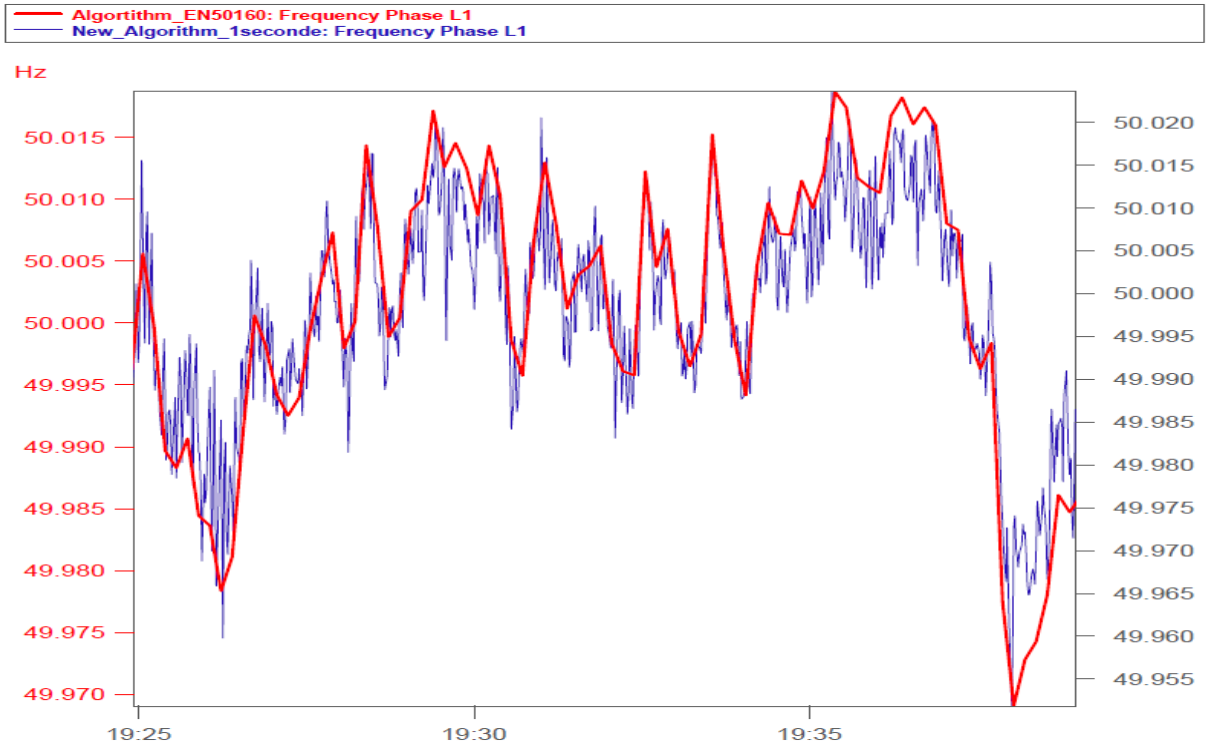

Figure 16. L1 voltage frequency recording (Zoom).

7. Conclusions

This paper explores the impact of voltage imbalance on three-phase networks and associated loads, specifically in the context of railway systems supplying 2 × 25 kV 50 Hz substations for high-speed trains. A quarterly experimental measurement of the voltage imbalance generated by these substations has been established for analysis due to the unique characteristics of these biphasic networks.

Experimental data from the Q80 power quality meter, based on the EN 50160 standard and installed at the 225 kV station, demonstrates a proportional relationship between the evolution of voltage imbalance and the load demand of high-speed trains. This substantiates the theoretical framework and calculations presented.

Further analysis involves the acquisition and evaluation of voltage imbalance with a variable integration period over which measurements are calculated. This approach shows enhanced accuracy in assessing voltage imbalance quantities, particularly in tracking time-varying inverse voltage components. This ensures the provision of adequate power quality and mitigates the negative effects induced by the inverse component on the electrical system.

Consequently, the proposed experimentally validated integration time interval of 1 s for 50 Hz signals is recommended for future voltage imbalance measurement instruments on 2 × 25 kV 50 Hz networks.

Based on the analysis of voltage imbalance over seven recordings of high-speed train journeys, substantial evidence is presented to advocate for equipping new power quality meters with a variable integration period. This allows standardization committees to conduct preliminary experimental measurements using agile devices equipped with a flexible algorithm similar to the proposed one. These devices will subsequently play a crucial role in the development and validation of new standards tailored for networks and specific loads other than those in the railway sector. This approach undoubtedly aids relevant entities in making informed decisions during incidents or malfunctions.

To standardize the proposed method and ensure its effectiveness across various traction networks and power systems, selecting the appropriate integration period for evaluating each power quality parameter and specific network is essential. This approach leads to

adaptive evaluations based on the integration period over which they are calculated, rather than absolute evaluations.

In conclusion, incorporating a variable integration period, as opposed to a fixed one, significantly enhances the analysis's adaptability and precision. It allows for more tailored data processing, matching the pace of parameter changes within the electrical network. This flexibility ensures that experts can adjust the analysis to capture rapid fluctuations or observe longer-term trends without losing detail or accruing unnecessary data. This adaptability not only improves the accuracy of power quality assessments but also optimizes the monitoring system's responsiveness to diverse operational conditions, enhancing its effectiveness in maintaining system integrity and compliance.

Author Contributions: Conceptualization, Y.T. and A.A.; Methodology, Y.T., R.L. and A.A.; Software, Y.T.; Validation, Y.T. and R.L.; Formal analysis, Y.T. and R.L.; Investigation, Y.T. and A.A.; Resources, Y.T.; Writing—original draft, Y.T. and R.L.; Writing—review & editing, Y.T., R.L. and A.A. All authors have read and agreed to the published version of the manuscript.

Funding: This research received no external funding.

Data Availability Statement: Data is unavailable due to privacy.

Conflicts of Interest: The authors declare no conflict of interest.

References

1. Zaré, M.; Varjani, A.Y.; Dehghan, S.M.; Kavehei, S. Compensation de la qualité de l'énergie et contrôle du flux de puissance dans les systèmes électriques de traction ferroviaire à courant alternatif. In Proceedings of the Dans les Actes de la 10e Conférence Internationale sur L'électronique de Puissance, les Systèmes D'entraînement et les Technologies (PEDSTC), Shiraz, Iran, 12–14 February 2019; pp. 426–432. (In French)
2. Huang, S.R.; Chen, B.-N. Etude harmonique du transformateur Le Blanc pour le système d'électrification des chemins de fer de Taiwan. *IEEE Trans. Power Del.* **2002**, *17*, 495–499. (In French)
3. Kryukov, A.V.; Cherepanov, A.V.; Shafikov, A.R. Modélisation des modes non sinusoïdaux dans les réseaux électriques alimentant les sous-stations de traction pour le fonctionnement des électromoteurs avec des convertisseurs à quatre quadrants. In Proceedings of the Dans Actes de la Conférence Internationale de L'oural 2019 Sur L'ingénierie de L'énergie Electrique (UralCon), Chelyabinsk, Russia, 1–3 October 2019; pp. 394–398. (In French)
4. Gazafrudi, S.; Langerudy, A.T.; Fuchs, E.; Al-Haddad, K. Power quality issues in railway electrification: A comprehensive perspective. *IEEE Trans. Ind. Electron.* **2015**, *62*, 3081–3090. [CrossRef]
5. Song, K.; Mingli, W.; Yang, S.; Liu, Q.; Agelidis, V.G.; Konstantinou, G. High-Order Harmonic Resonances in Traction Power Supplies: A Review Based on Railway Operational Data, Measurements and Experience. *IEEE Trans. Power Electron.* **2019**, *35*, 2501–2518. [CrossRef]
6. Taleb, Y.; Lamrani, R.; Abbou, A. Study of the Current Harmonics Generated by Two-Phase Loads on HV Transmission Power Grid: A Case Study of a Substation Supplying the High-Speed Rail. *Int. Rev. Electr. Eng.* **2023**, *18*, 265–274. [CrossRef]
7. Cheok, A.D.; Kawamoto, S.; Matsumoto, T.; Obi, H. High power AC/DC converter and DC/AC inverter for high speed train applications. In Proceedings of the 2000 TENCON Proceedings. Intelligent Systems and Technologies for the New Millennium (Cat. No. 00CH37119), Kuala Lumpur, Malaysia, 24–27 September 2000; Volume 1, pp. 423–428.
8. Matta, V.; Kumar, G. Unbalance and voltage fluctuation study on AC traction system. In Proceedings of the 2014 Electric Power Quality and Supply Reliability Conference (PQ), Rakvere, Estonia, 11–13 June 2014; pp. 303–308.
9. Hu, H.; Shao, Y.; Tang, L.; Ma, J.; He, Z.; Gao, S. Overview of Harmonic and Resonance in Railway Electrification Systems. *IEEE Trans. Ind. Appl.* **2018**, *54*, 5227–5245. [CrossRef]
10. Frelin, W. Impact de la Pollution Harmonique sur les Matériels de Réseau. Energie Electrique. Ph.D. Dissertation, Université Paris Sud—Paris XI, Bures-sur-Yvette, France, 2009.
11. Seferi, Y.; Blair, S.M.; Mester, C.; Stewart, B.G. Power Quality Measurement and Active Harmonic Power in 25 kV 50 Hz AC Railway Systems. *Energies* **2020**, *13*, 5698. [CrossRef]
12. Féminin, A.D.; Gallo, D.; Giordano, D.; Landi, C.; Luiso, M.; Signorino, D. Évaluation de la qualité de l'énergie dans les systèmes d'alimentation en traction ferroviaire. *IEEE Trans. Instrum. Mes.* **2020**, *69*, 2355–2366. (In French)
13. Féminin, A.D.; Gallo, D.; Landi, C.; Luiso, M. Discussion sur l'évaluation de la qualité de l'alimentation CC et CA dans les systèmes d'alimentation en traction ferroviaire. In Proceedings of the Dans les Actes de la Conférence Internationale sur les Technologies D'instrumentation et de Mesure de l'IEEE 2019 (I2MTC), Auckland, New Zealand, 20–23 May 2019; pp. 1–6.
14. Diaz, J.A.S. Etude et modelisation des interactions electriques entre les engins et les installations fixes de traction electrique 25 kV 50 Hz. Ph.D. Thesis, Université de Toulouse, Labège, France, 2014. (In French).

15. Laaksonen, H.; Parthasarathy, C.; Hafezi, H.; Shafie-khah, M.; Khajeh, H. Control and Management of Distribution Networks with Flexible Energy Resources. *Int. Rev. Electr. Eng.* **2020**, *15*, 2–3. [CrossRef]
16. *CEI 61000-4-30:2015*; Compatibilité Electromagnétique (CEM)—Partie 4-30: Techniques de Test et de Mesure—Méthodes de Mesure de la Qualité de L'énergie. Commission Electrotechnique Internationale: Genève, Suisse, 2015. (In French)
17. *CEI 61000-4-7*; Compatibilité Electromagnétique (CEM)—Partie 4-7: Techniques D'essai et de Mesure—Guide Général sur Les mesures et L'instrumentation des Harmoniques et des Interharmoniques, Pour les Systèmes D'alimentation Electrique et les Equipements Qui y Sont Connectés. Commission Electrotechnique Internationale: Genève, Switzerland, 2008. (In French)
18. Bouzbiba, A.; Taleb, Y.; Abbou, A. Realization of an Electrical Power Quality Analyzer Based on NIDAQ6009 Board. In *Digital Technologies and Applications, Proceedings of the International Conference on Digital Technologies and Applications*; Fez, Morroco, 27–28 January 2023, Lecture Notes in Networks and Systems; Motahhir, S., Bossoufi, B., Eds.; Springer: Cham, Switzerland, 2023; Volume 668. [CrossRef]
19. ANSI/NEMA Standard MG1-1993. Motors and Generators. Available online: https://webstore.ansi.org/standards/nema/nemamg1993 (accessed on 2 February 2024).
20. *IEEE Standard 112*; IEEE Standard Test Procedure for Polyphase Induction Motors and Generators. IEEE: New York, NY, USA, 1991.
21. Dugan, R.C.; McGranaghan, M.F.; Beaty, H.W. *Electrical Power Systems Quality*; McGraw-Hill: New York, NY, USA, 1996.
22. von Jouane, A.; Banerjee, B. Assessment of voltage unbalance. *IEEE Trans. Power Deliv.* **2001**, *16*, 782–790. [CrossRef]
23. Assefa, S.A.; Kebede, A.B.; Legese, D. Harmonic analysis of traction power supply system: Case study of Addis Ababa light rail transit. *IET Electr. Syst. Transp.* **2021**, *11*, 391–404. [CrossRef]
24. Etxeberria, I.; Viscarret, U.; Caballero, M.; Rufer, A.; Bacha, S. New Optimized PWM VSC Control Structures and Strategies Under Unbalanced Voltage Transients. *IEEE Trans. Ind. Electron.* **2007**, *54*, 2902–2914. [CrossRef]
25. Vekhande, V.; Pimple, B.B.; Fernandes, B.G. Modulation of Indirect Matrix Converter under unbalanced source voltage condition. In Proceedings of the Energy Conversion Congress and Exposition (ECCE), Phoenix, AZ, USA, 17–22 September 2011; pp. 225–229.
26. Chen, T.-H. Evaluation of line loss under load unbalance using the complex unbalance factor. *IEE Proc.-Gener. Transm. Distrib.* **1995**, *142*, 173–178. [CrossRef]
27. Ansari, A.A.; Deshpande, D.M. Investigation of performance of 3-phase Asynchronous machine under voltage unbalance. *J. Theor. Appl. Inf. Technol.* **2009**, *6*, 22.
28. Dang, X.-L.; Hoang, E.; Ahmed, H.B.; Petit, M.; Pham, H.T. Etude de l'équilibrage des courants de phases par convertisseur statique dans un réseau de distribution. In Proceedings of the Journées JCGE'2014—SEEDS, Saint-Louis, France, 4–5 June 2014. (In French).
29. Chen, T.-H. Comparison of Scott and Leblanc transformers for supplying unbalanced electric railway demands. *Electr. Power Syst. Res.* **1994**, *28*, 235–240. [CrossRef]
30. Kersting, H.W. Causes and Effects of Unbalanced Voltages Serving an Induction Motor. *IEEE Trans. Ind. Appl.* **2010**, *37*, 165–170. [CrossRef]
31. Bhavaraju, V.B.; Enjeti, P.N. Analysis and design of an active power filter for balancing unbalanced loads. *IEEE Trans. Power Electron.* **1993**, *8*, 640–647. [CrossRef]
32. Ghosh, A.; Joshi, A. A new approach to load balancing and power factor correction in power distribution system. *IEEE Trans. Power Deliv.* **2000**, *15*, 417–422. [CrossRef]
33. Chen, C.-C.; Hsu, Y.-Y. A novel approach to the design of a shunt active filter for an unbalanced three-phase four-wire system under nonsinusoidal conditions. *IEEE Trans. Power Deliv.* **2000**, *15*, 1258–1264. [CrossRef]
34. Plummer, I. Asymmetry in Distribution Systems: Causes, Harmful Effects and Remedies. Master's Thesis, Luisiana State University, Baton Rouge, LA, USA, 2011; 138p.